informes de la construcción

Informes de la Construcción 77 (578)
abril-junio 2025, 6921
ISSN-L: 0020-0883, eISSN: 1988-3234
https://doi.org/10.3989/ic.6921

Analytical modelling and the minimum thickness of three-centred arches

Modelización analítica y espesor mínimo de arcos de tres centros

Dimitriye Nikolich

University of Novi Sad, Faculty of Technical Sciences. Serbia.
Autor de contacto: dima@uns.ac.rs

ABSTRACT

Equilibrium analyses of vaulted masonry structures, as well as the mathematical modelling of their structural behaviour, have gained prominence within researches on both historic structures and novel digitally fabricated designs. Thus, by revisiting the classical problem of limit equilibrium states determination, minimum thicknesses necessary to secure stability for the most common arch shapes have been recently computed. However, three-centred or basket-handle arch, which was prevalent in Renaissance architecture in the form of classic ovals, has not yet received the deserved attention in terms of its structural behaviour. Therefore, the present research addresses this gap by developing the analytical model for such arches according to thrust line theory. Numerical calculations carried out are based on the five-hinged collapse mode and provide the exact and valuable insights into the correlation between arch shape and the required minimum thickness, which is graphically presented for more than thirty arches.

Keywords: basket-handle arch; limit equilibrium analysis; thrust line; oval; minimum thickness.

RESUMEN

Los análisis de equilibrio de estructuras abovedadas de fábrica *y la modelización matemática de su comportamiento estructural han ganado prominencia en investigaciones sobre estructuras históricas y diseños digitalmente fabricados. Al volver a examinar el problema clásico de la determinación de estados de equilibrio límite, recientemente se han calculado los espesores mínimos necesarios para garantizar la estabilidad de las formas de arco más comunes. Sin embargo, el arco de tres centros o arco carpanel, predominante en la arquitectura renacentista en forma de óvalos clásicos, no se analiza estructuralmente con suficiente detalle. Por lo tanto, la presente investigación desarrolla el modelo analítico para tales arcos según la teoría de la línea de empuje. Los cálculos numéricos realizados, basados en el modo de colapso de cinco bisagras, proporcionan la correlación exacta entre la forma del arco y el espesor mínimo requerido, que se presenta gráficamente para más de treinta arcos.*

Palabras clave*: arco carpanel; análisis de equilibrio límite; línea de empuje; oval; mínimo espesor.*

Cómo citar este artículo/Citation: Dimitriye Nikolich (2025). Analytical modelling and the minimum thickness of three-centred arches. Informes de la Construcción, 77 (578): 6921. https://doi.org/10.3989/ic.6921

Recibido/*Received*: 26/02/2024
Aceptado/*Accepted*: 03/03/2025
Publicado on-line/*Published on-line*: 24/11/2025

1. INTRODUCTION

Ancient builders invented various forms of construction elements in order to cover a space, i.e., to span openings in the wall or between columns. Lintels or monolithic stone blocks, used in the architrave construction system, evolved to vaulted masonry structures, which today represent a large part of architectural heritage. Therefore, various mathematical or computational models aimed for stability and safety analysis are created in order to predict and prevent possible collapse. However, for a very long period, dimensioning followed purely geometrical rules of construction based solely on experience and intuition, rather than the knowledge of structural mechanics (1-3). Thus, Vitruvius' firmitas primarily belongs to the field of geometry (4), since a shape is the one that provides the stability of a structure. From Hooke's well-known anagram (5, 6) onwards, scholars, architect and engineers strive to adapt a structure shape and a material used for its erection to a corresponding loading and force transmission, thereby creating novel structure forms as well as models which better describe the structure behaviour (7). Although considered earlier, it was Couplet (8) who first stated precise assumptions about material behaviour, and introduced collapse modes, i.e., possible mechanisms caused by the formations of rupture joints (cracks) or so-called hinges, as the basis of the analysis of arch failure (9). Consequently, he tried to determine a theoretical minimum thickness of a uniform semicircular arch subjected to its own weight—today known as Couplet's problem.

The concept of thrust line, introduced by Young (10, 11) at the beginning of the nineteenth century, and elaborated by Moseley (12), enabled the graphical visualization of a load path (line of resistance) through an arched structure. Accordingly, the thrust line is defined as the locus of application points of resultant thrust forces that develop at joints (beds) between voussoirs of an arch. This provided complete insight into relation between a structure geometry and the corresponding force flow; hence, a mechanical problem of structural stability reduced to a mainly geometrical task, whereby the self-weight of a finite arch portion is substituted by the corresponding area of the arch ring, and is applied in the corresponding centre of gravity. Further, the theory of masonry arches made a full circle: starting from so-called classic or old theory reflected in graphical statics epoch developed systematically by Culmann (13) in the second half of the nineteenth century; passed through elastic theory phase in the first half of the twentieth century; and fit within the general field of plastic theory, i.e., limit analysis. The latter enabled the so-called equilibrium approach (or geometric formulation) reflected in simple statics in the sense of the theory of statically determined systems (14, 15). Finally, it was Serbian scholar Milutin Milankovitch who, more than a century ago, treated the thrust line concept (Druckkurven) in the most rigorous manner, and set the complete and correct theory for the equilibrium analysis of a masonry arch of general (curved) shape. Hence, after remarkable mathematical elaboration, provided in for a long period nearly unknown work (16, 17), he was the first who gave the theoretically correct solution to Couplet's problem, which recently influenced today's researchers to extend the problem to other common arch shapes (18, 19). Thus, revisiting the classical issue of determining the limit equilibrium states, based on Milankovitch's approach, the analysis has been extended on both incomplete (segmental) and overcomplete (horseshoe) circular (20), semi-elliptical (21) and pointed arches (22).

In addition, various analytical procedures, based on different methods, such as geometric formulation (16, 18, 22-24), variational formulation (18, 21, 25) and stability area method (26, 27), are proposed. Furthermore, by adapting the theory of thrust line to different numerical procedures (22, 28-32) that involves the modelling of an arch as a discretized system of large number of voussoirs of a finite size, a variety of structural software for the analysis of thrust line, minimum thickness or collapse mechanism, aimed for different arch shapes and loading conditions, are recently developed (33-38). Nonetheless, for arches of regular shape, such are circular-based ones, a simple analytical modelling of a thrust line, based on a geometric formulation and combined with a basic iterative procedure (22), provides a direct approach to obtaining a value and a visualization of minimum thickness.

Among the mentioned arch shapes, within objects of architectural heritage, common are arches of ellipse-like shape. Elliptical shape requires more complex procedures of forming the voussoirs and construction, and thus is approximately represented by ovals which consist of several circular arcs. Starting from Serlio (39) (Figure 1e and Table 2), geometric construction of ovals became popular during the renaissance period within architecture and carpentry or stereotomy treatises (40-44).

Although there are examples for circular-based arches composed of five, seven, or even eleven constituent parts (45, 46), the most common ones are composed of three parts: so called three-centred or basket-handle arches (Figure 1). They can be found from some of niches in Vatican grottoes to entrance doors within modernist architecture, and are of particular interest in the present research. Namely, such a symmetrical arch represents a system of three annuli (circular ring) sectors, i.e., it is consisted of one upper (inner, central) part of radius R and two lower (outer, lateral) parts of radius r, as shown in Figure 2 (when the radii are equal, the semicircular arch is obtained). Accordingly, two cases are possible: (i) depressed (surbased) three-centred arch in which the upper part is of larger radius than the lower one (Figure 2b), and (ii) raised three-centred arch, which is rarer and in which the lower part is larger than the upper one (Figure 2c).

Arches of the first type are particularly present in Spanish or French renaissance architecture, e.g., within castles of the Loire group (Château de Chenonceau (Figure 1a), Royal Château de Blois) or in Hôtel de Ville (The Town Hall) in Arles (47, 48). In addition, due to suitable shape, they are used in bridge design (e.g., George V Bridge over the Loire River in Orléans (Figure 1b) or in some of the New York Central Park bridges).

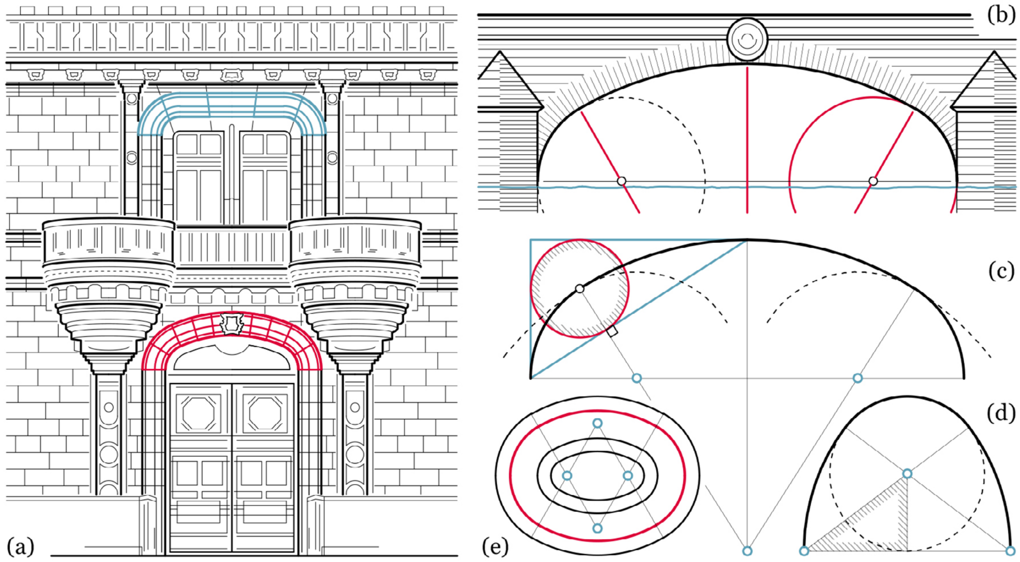

Figure 1. Three-centred arches: (a) entrance to the Château de Chenonceau, (b) George V Bridge across the Loire in Orléans, (c) optimal oval construction according to (31), (d) Egyptian vault shape, (e) Serlio's sketch for oval layout

The second arch type can be found in traditional Egyptian vault construction, e.g., when the particular ratio between radii of the circular parts is based on the Pythagorean right-triangle, as shown in Figure 1d. In addition, if the radius of the upper (central) part of the arch is infinitely large, a flat (straight, horizontal) part is obtained instead of the segmental (circular) one, and thus a pseudo-three-centred arch is formed. It is used, for example, instead of lintels above windows (Figure 1a) or within flattened vaults above long galleries.

Although three-centred arches are commonly present in historic structures, their structural behaviour is not examined in sufficient detail. Aita et al. (26) considered two arches bearing a vertical wall according to stability area method and nonlinear elastic analysis. However, most research primary focused on geometrical properties of such arches omitting a corresponding structural framework. Thus, a particular shape, in which the transition joint passes through the incentre of the inscribed circle of the right-angled triangle defined by the crown and springing point (as shown in Figure 1c), is referred as the optimal one regarding both aesthetic and structural criteria in (47). The present paper aims to develop the model for the equilibrium analysis of such arches and to correlate the arch shape to the corresponding minimum thickness.

2. METHODS

The basis of the consideration carried out in the present research is thrust line theory. Accordingly, the geometric (equilibrium) approach is applied in static analysis. In accordance with the usual (so-called Couplet's or Heyman's) assumptions, it has been adopted that the masonry material from which the arch is made has the following properties: (a) unlimited compressive strength, (b) zero tensile strength, and (c) no slippage (unlimited friction). Therefore, the arch is considered to be solid continuous (monolithic) and homogeneous body without tensile strength, while pressure is transmitted in all directions within boundaries (unilateral material). Three-centred and pseudo-three-centred arches of constant (uniform) thickness subjected only to self-weight are considered, and due to the symmetry of arches, only a half-arch is analysed. According to the presented theoretical background, the methodological framework is as follows.

Analytical modelling:

– The upper part of a three-centred arch is acting as a half of a segmental (circular) arch, while its lower part is acting as an annulus sector (circular ring sector); hence the normal stereotomy which considers generic sections perpendicular to the midline (axis) of the arch is applied. Since

the joints within each part are directed radially from the corresponding centre, two independent polar coordinate systems, having origins coincident with the centre of the corresponding part, are adopted for the analysis, as one can see in Figure 2a. With reference to the part within the generic (arbitrary) section (defined by the angle φ) is located, the analysis is conducted.
– For a pseudo-three-centred arch, the straight (central) part is acting as a flat (jack) arch, while the circular part is acting as the one half of the semicircular arch (annuli sector of right embrace angle). Since, within a flat arch, a critical section at intrados (i.e., a mechanism of collapse) cannot occur, it is sufficient to analyse the equilibrium of the lower (circular) part under the influence of the load from the upper (flat) part.
– Five-hinged collapse mode, valid for elliptical arches, is adopted due to shapes similarity. Thus, out of an infinite number of physically admissible thrust lines, in order for the arch to be a statically determined system, one is chosen uniquely by selecting three points the thrust line passes through: extrados points of the crown joint and two springing joints.
– Identification of the particular geometric parameters of thrust line: (i) weight of the finite portion of the arch, and (ii) the corresponding centre of gravity. The unit value is adopted for the specific weight of material and the width (depth) of an arch; thus, a self-weight of the arch or its portion is substituted by the area of the corresponding arch sector, limited by extrados and intrados curves and by particular joints between voussoirs; then, it is applied in the centre of gravity, i.e., in the centroid of the limited area.
– Determination of the horizontal thrust from the rotational equilibrium about the springing hinge (the application point of reaction force).
– Derivation of the closed-form expression of the thrust line from rotational equilibrium about the application point of resultant thrust force at a generic section.

Numerical modelling and thrust line analysis:
– Since the collapse mode is defined, as well as the position of thrust line at the crown and springings, in order to attain the limit equilibrium state, only the intrados hinge requires a determination. This involves an iterative procedure by which the thickness of the arch is reduced until the thrust line touches the intrados (up to the required level of accuracy), and is conducted according to the method provided in (22).
– Computation of numerical values for various arch shapes, represented by the ratio between radii of upper and lower parts and the value of transition angle (embrace angle of upper part), and establishing the graphical correlation between the geometric properties of an arch and its possible minimum thickness.

3. ANALYTICAL MODELLING

In order to apply a geometric formulation (static approach), which concerns the derivation of thrust line expression and its analysis, geometrical properties of the annulus sector have to be thoroughly treated.

3.1 Three-centred arches

Geometrical parameters of the right half of a three-centred arch of uniform thickness *t* are shown in Figure 2a. The arch axis (midline) is defined by the half-span *l*, the height *h*, and the transition angle α between the upper part I (centre O, radius *R*) and the lower part II (centre C, radius *r*). The vertical distance between the upper part centre O and the springing line is defined by the following relation: $d = (l-r)\cot\alpha$. With reference to Figure 2b,c, based on expressions sin α = *l*−*rR*−*r* and $h = R-d$, one can derive the relation between the lower part radius *r* and the arch axis parameters *l*, *h* and α:

$$[1] \quad r = \frac{h \sin\alpha + l\,(\cos\alpha - 1)}{\sin\alpha + \cos\alpha - 1}$$

The angle φ is angular coordinate which defines a generic section, and is measured from the vertical axis of the symmetry of the arch (values of the angle φ within intervals [0, α] and [α, π/2] correspond to part I and part II, respectively). Hence, if a generic section lies within part I having the radius *R*, the corresponding weight V_1 of the finite arch portion (between the crown joint and the generic section) is represented by the area of the corresponding annulus sector (Figures 2a and 3a), and is expressed by:

$$[2] \quad V_1(\varphi) = R\,t\,\varphi$$

When the generic section reaches the end of part I, that is, when the value of the angle φ reaches the value of the embrace angle α, the weight *W*1 of part I is obtained:

$$[3] \quad W_1 = V_1(\varphi = \alpha) = R\,t\,\alpha$$

On the other side, if the generic section is located within part II of the radius r (Figures 2a and 3b), the corresponding area $V2$, between the transition joint at the angle α and a generic section at the angle φ, is given by:

$$[4]\ \ V_2(\varphi) = r\,t\,(\varphi - \alpha)$$

The weight $W2$ of part II is obtained when the angle φ reaches value $\pi/2$:

$$[5]\ \ W_2 = V_2(\varphi = \pi/2) = \ r\,t\,(\pi/2 - \alpha)$$

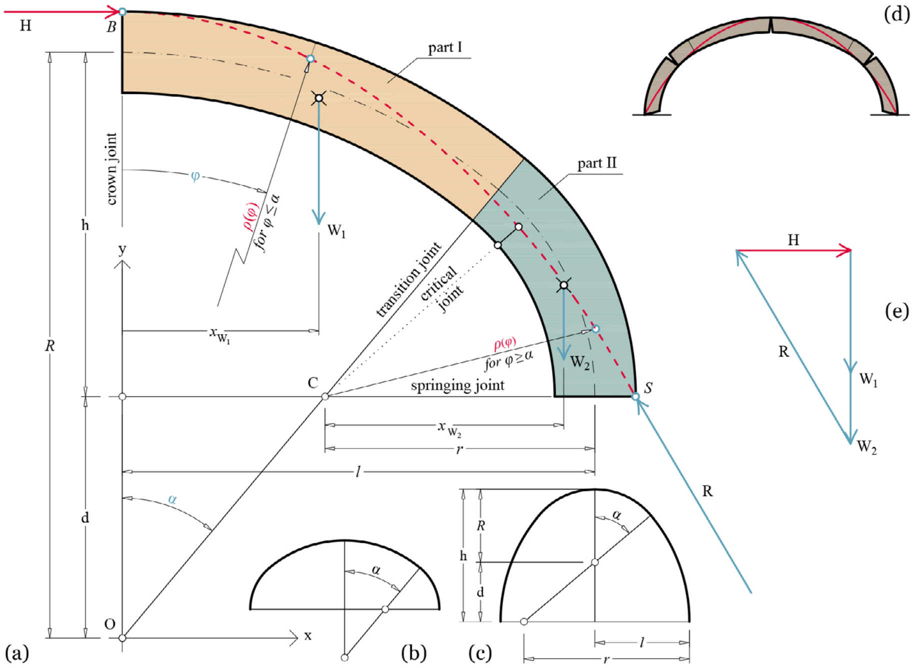

Figure 2. Three-centred arch: (a) geometrical parameters, (b) depressed three-centred arch (R > r), (c) raised three-centred arch (R < r), (d) collapse mode, (e) force plan

In accordance with previous expressions, considering the location of a generic section, the weight of a finite arch portion is defined by following expressions:

$$[6a]\ \ V(\varphi) = V_1(\varphi) = R\,t\,\varphi \qquad \text{for } 0 < \varphi \le \alpha$$

$$[6b]\ \ V(\varphi) = W_1 + V_2(\varphi) = R\,t\,\alpha + r\,t\,(\varphi - \alpha) \qquad \text{for } \alpha < \varphi \le \pi/2$$

The abscissa x_{V_1} of the centroid of a finite arch portion (annulus sector) up to the angle φ within part I is given by:

$$[7]\ \ x_{V_1}(\varphi) = \frac{4}{3}\,\frac{R_{ex}^3 - R_{in}^3}{R_{ex}^2 - R_{in}^2}\,\frac{\sin\left(\frac{\varphi}{2}\right)}{\varphi} = \frac{(12R^2+t^2)(1-\cos\varphi)}{12R\varphi}$$

where $R_{ex} = R+t/2$ and $R_{in} = R-t/2$ are radii of extrados and intrados, respectively. Similarly, the abscissa x_{V_2} of the centroid of the area $V2$ within part II is following:

$$[8]\ \ x_{V_2}(\varphi) = \frac{4}{3}\,\frac{r_{ex}^3 - r_{in}^3}{r_{ex}^2 - r_{in}^2}\,\frac{\sin\frac{\alpha+\varphi}{2}}{\varphi-\alpha}\ \sin\frac{\alpha+\varphi}{2} = \frac{(12r^2+t^2)(\cos\varphi - \cos\alpha)}{12r(\alpha-\varphi)}$$

where $r_{ex} = r + t/2$ and $r_{in} = r - t/2$ are radii of extrados and intrados, respectively. When the angle φ reaches the value α, the abscissa x_{W_1} of the centroid of part I is obtained:

$$[9]\ \ x_{W_1} = \frac{(12R^2+t^2)(1-\cos\alpha)}{12R\alpha}$$

and when the angle φ reaches value $\pi/2$, the abscissa x_{W_2} of the centroid of part II is obtained:

$$[10]\ \ x_{W_2} = \frac{(12r^2+t^2)\cos\alpha}{12r(\pi/2-\alpha)}$$

Accordingly, the abscissa x_V of the centroid of the finite arch part having the weight V, between the crown joint and the generic section up to the angle φ, can be computed according to the following expressions:

[11a] $x_V(\varphi) = x_{V_1}(\varphi) = \frac{(12R^2+t^2)\ (1-cos\ \varphi\ )}{12R\varphi}$ for 0 < φ ≤ α

[11b] $V(\varphi) = W_1 + V_2(\varphi) = Rt\alpha + rt(\varphi-\alpha) = \frac{6\pi r^2-6\alpha\left[2r^2+rt-R(2l+t)\right]+3\pi rt-12\left(r^2-R^2\right)cos\ \alpha\ -12R^2-t^2}{(R-r)\alpha+r\varphi}$
for α < φ ≤ π/2

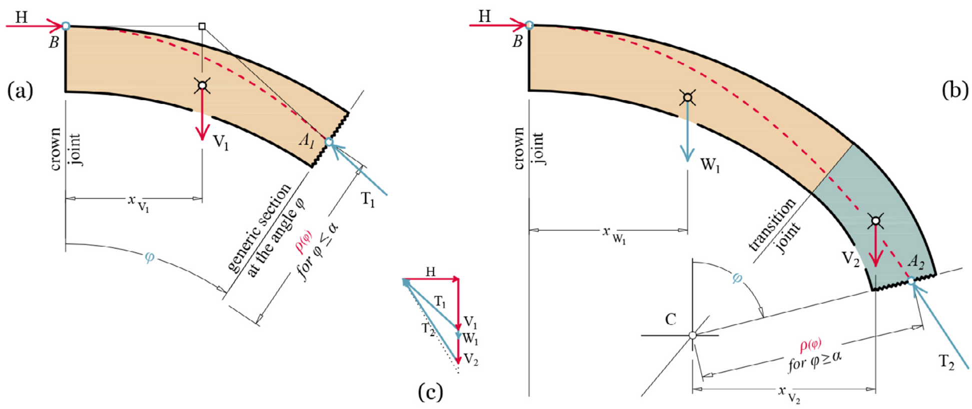

Figure 3. Equilibrium of a finite top arch portion up to the generic section at the angle φ: (a) within part I, (b) within part II, (c) force polygon

As stated, the application point B of the horizontal force H at the crown and the application point S of the reaction force R at the springing are set at the extrados. From the rotational equilibrium of a half-arch about the springing hinge S, one can determine the expression describing the value of horizontal thrust acting at the crown:

[12] $H = \frac{W_1(l+\frac{t}{2}-x_{w_1})+W_2(r+\frac{t}{2}-x_{w_2})}{h+\frac{t}{2}} = \frac{t\ \{\ 6\pi r^2-6\alpha\left[2r^2+rt-R(2l+t)\right]+3\pi rt-12\left(r^2-R^2\right)cos\ \alpha\ -12R^2-t^2\ \}}{6\ (2h+t)}$

Further, the resultant thrust force T at the generic section at the angle φ together with its point of application A is uniquely defined from the force and moment equilibrium of the finite arch portion. According to Figure 3, rotational equilibrium about the point A is given by the following equality: $H\ (R_{ex} - \rho \cos\varphi) = V(\varphi)\ (\rho \sin\varphi - x_V(\varphi))$, on the base of which follow expressions which describe thrust line:

[13a] $\rho(\varphi) = \frac{V(\varphi)x_V(\varphi)+H(R+\frac{t}{2})}{V(\varphi)sin\ \varphi\ +Hcos\ \varphi}$ for 0 < φ ≤ α

[13b] $\rho(\varphi) = \frac{V(\varphi)(r-l+x_V(\varphi))+H(h+\frac{t}{2})}{V(\varphi)sin\ \varphi\ +Hcos\ \varphi}$ for α < φ ≤ π/2

where V(φ), x_V (φ) and H are given by Eqs. [6], [11] and [12], respectively. Eq. [13a] defines the distance ρ between the thrust line within part I and the corresponding centre O, while Eq. [13b] is the distance ρ from the thrust line within part II to the corresponding centre C (cf. Figures 2 and 3).

3.2. Pseudo-three-centred arches

One half of a pseudo-three-centred arch, consisted of the straight part I (weight $W1$) and the circular part II (weight $W2$), is shown in Figure 4, where geometric parameters are marked. For arches of uniform vertical thickness under the vertical stereotomy, the thrust line is of parabolic shape (10, 49). That can be applied for straight part I, and the corresponding analysis can be omitted. Hence, only part II, on which the resultant thrust force from the upper part I acts, is analysed. A polar coordinate system with the origin coincident with the centre C of the quarter-circle is adopted. The location of the application point M of the resultant force (the components of which are the vertical force $W1$ and the horizontal thrust H, as shown in Figure4 c,d) at the transition joint can be determined from the rotational equilibrium of part I about the point M. It is defined by the vertical distance q_M from the extrados, given by the following expression:

[14] $q_M = \frac{W_1}{H}\frac{l-r}{2}$

The weight $W1$ of the flat part I (represented by the rectangular area) and the weight $W2$ of the circular part II (represented by the quarter of annulus) are given by following expressions:

[15a] $W_1 = t\ (l-r)$

[15b] $W_2 = r\,t\,\frac{\pi}{2}$

while abscissas x_{W1} and x_{W2} of corresponding centroids, respectively, are:

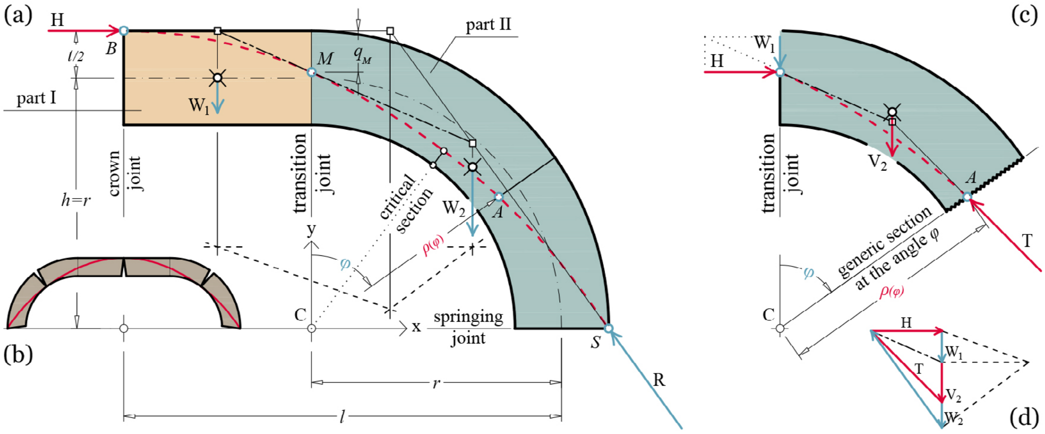

Figure 4. Pseudo-three-centred arch: (a) geometrical parameters, (b) collapse mode, (c) finite segment of part II from the transition joint up to the generic section at the angle φ, (d) force polygon

[16a] $x_{W_1} = \frac{l-r}{2}$

[16b] $x_{W_2} = \frac{4\left(R_{ex}^3 - R_{in}^3\right)}{3\pi\left(R_{ex}^2 - R_{in}^2\right)}$

The weight V of the finite arch portion within part II, from the vertical transition joint up to the generic section at the angle φ, and the corresponding abscissa x_V of the centre of gravity, similarly to Eqs. [2] and [7], respectively, are given by:

[17a] $V(\varphi) = r\,t\,\varphi$

[17b] $x_V(\varphi) = \frac{(12r^2+t^2)(1-\cos\varphi)}{12r\varphi}$

Rotational equilibrium about the point S is expressed by the following equality:

[18] $H\left(r + \frac{t}{2}\right) = W_1\left(l + \frac{t}{2} + x_{W_1}\right) + W_2\left(r + \frac{t}{2} + x_{W_2}\right)$

where values $W1$, $W2$, x_{W1} and x_{W2} are given by Eqs. [15a], [15b], [16a] and [16b], respectively. Thus, the horizontal thrust value H can be expressed:

[19] $H = \frac{t\left[6l^2+6lt+6r^2(\pi-3)+3rt(\pi-2)-t^2\right]}{6(2r+t)}$

As stated, within part I, the thrust line has the shape of a parabola, while the expression that describes the thrust line within part II is reduced from the rotational equilibrium about the point A:

[20] $\rho(\varphi) = \frac{V(\varphi)x_V(\varphi)+H\left(r+\frac{t}{2}-q_M\right)}{(W_1+V(\varphi))\sin\varphi + H\cos\varphi}$

where values q_M, $W1$, $V(\varphi)$, $x_V(\varphi)$ and H are given by Eqs. [14], [15a], [17a], [17b] and [19], respectively.

4. NUMERICAL MODELLING

Since three-centred arches have a smooth (circular) crown, when the limit equilibrium state is assumed, the arrangement of hinges (critical sections) resembles the collapse mode of a semicircular or elliptical arch (Figure 2d). The thrust line which corresponds to the arch of minimum thickness passes through extrados both at the crown and springings, touching intrados in two unknown points, theoretically forming five hinges. Accordingly, for the determination of the minimum thickness, it is sufficient to analyse the position of the thrust line with respect to the intrados.

Within a three-centred arch, the hinge at intrados can occur within the upper part I or the lower part II, depending of the ratio of their radii. Hence, for each generic section, the distance from thrust line to the intrados, δ_{in}, is defined by the following expressions:

[21a] $\delta_{in}(\varphi) = \rho(\varphi) - R_{in}$ for the upper arch part, i.e., for $0 < \varphi \leq \alpha$

[21b] $\delta_{in}(\varphi) = \rho(\varphi) - r_{in}$ for the lower arch part, i.e., for $\alpha < \varphi \leq \pi/2$

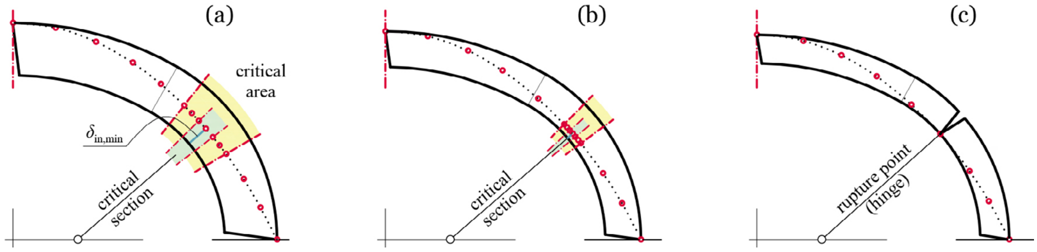

Figure 5. Critical area selection: (a) initial arch (sub)division, (b) gradual narrowing of the critical area, (c) limit equilibrium state

where R_{in} and r_{in} are radii of intrados of the upper and lower part, respectively, and the value $\rho(\varphi)$ is given by Eq. [13]. Since, in the case of pseudo-three-centred arch, the hinge at the intrados can occur only within the lower (quad-circular) part, the distance δ_{in} is given by:

[22] $\delta_{in}(\varphi) = \rho(\varphi) - r_{in}$

where the value $\rho(\varphi)$ is given by Eq. [20]. In order to determine minimum thickness and corresponding hinge at intrados, the iterative procedure regarding critical area selection developed in (22) can be adapted for three-centred and pseudo-three-centred arches. Namely, in preprocessing step, the half-arch is initially divided into three portions, as shown in Figure 5a, and each portion is subdivided into the appropriate number of segments regarding generic sections. Computed values δ_{in} are temporarily stored in appropriate lists. The critical section refers to the joint containing the minimal value $\delta_{in,min}$ within the list. Hence, in order to determine the limit state, sections neighbouring to the critical section define the critical area for the next iteration (Figure 5b), while the arch thickness from the previous iteration is modified according to the following rule:

[23] $t = t - \delta_{in,min}$

Hence, the thickness is decreased along with the gradual successive narrowing of the critical area, until the thrust line reaches the intrados up to a satisfactory precision (all the values have been computed with the minimum precision of 10^{-12}).

5. RESULTS

According to the guidelines, as well as expressions, provided in previous section, the computation for three-centred and pseudo-three-centred arches of various proportions is conducted, and the numerical values for the theoretical minimum thickness (represented by the ratio *t/l* between the arch thickness and its half-span) which correspond to limit equilibrium states are obtained.

For the computation, the proportions of three-centred arches are defined by the ratio *l:h* between half-span and the height of arch midline. Arches having transition angle α equal to 30, 45 and 60 degrees are considered, and computed numerical values of minimum thickness are provided in Table 1, along with the graphical representation of these arches, which correspond to limit equilibrium state (all the arches are of the same span).

Further, the location of the critical section (hinge which occurs at intrados) is specified by the angle β_{in}. One can see that for α = 30° and α = 45°, the hinge is located within (lower) part II, while for α = 60° it is within (upper) part I. Of particular interest are arches the midline of which has the shape of ovals of classic proportions, i.e., the well-known applied geometric constructions (43). Visual presentation of such ovals with their parameters, as well as the corresponding arches of minimum thickness with the corresponding thrust line and hinges arrangement are shown in Table 2.

In addition, on the base of the obtained numerical results, the correlation between minimum thickness and arch shape is traced in the diagram presented in Figure 6. One can see that for each of analysed transition angles, the graph is of parabola-like shape: starting from raised (narrow) arches, by increasing the elongation (*l:h*), the minimum thickness gradually increases and after a particular point it decreases. Thus, there is a range of proportions for which a greater thickness is required to provide a stable arch. The common (intersecting) point between shown curves corresponds to the semicircular arch (whereby *l:h = 1* and the value of transition angle has no effect).

On the base of values provided in (21), the minimum thickness of elliptical arches is traced by the dashed line. One can note that for the transition angle α=45°, the minimum thickness value of three-centred arches is in most cases smaller than the elliptical ones, while in cases when α=30° and α=60°, this relation is variable.

Considering classical oval proportions regarding depressed arches (cf. Table 2), the ones with α = 30° (e.g., Serlio's IV and Vignola's) turn out to be within the range of the maximum values of possible minimum thickness (t/l ≈ 0.12); such arches are consequently more unsuitable than elliptical arches of the same proportions, while the ones with α = 45° (Serlio's methods II and III) appear a little more suitable. On the other side, raised three-centred arches (e.g., Egyptian oval, that is, rotated Vignola's oval) are the most suitable regarding minimum thickness value (t/l ≈ 0.08).

Table 1. Three-centred arches of minimum thickness

	30°		45°		60°	
$l : h$	t/l	β_{in} [°]	t/l	β_{in} [°]	t/l	β_{in} [°]
0.60			0.06965	70.46	0.09534	56.08
			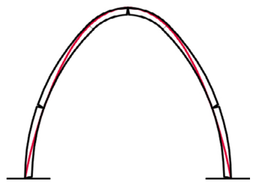		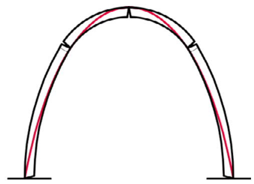	
0.75	0.08117	64.57	0.08819	63.15	0.11333	56.31
	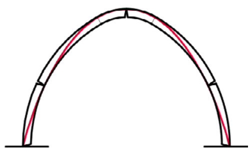		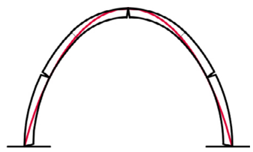		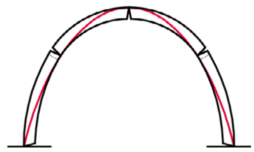	
1.00	0.10748	54.48	0.10748	54.48	0.10748	54.48
	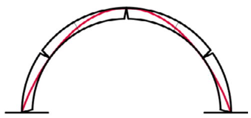		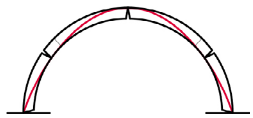		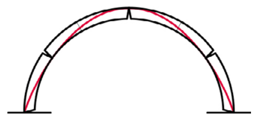	
1.25	0.12096	48.33	0.10618	50.59	0.08323	51.19
	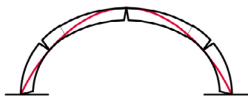		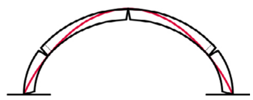		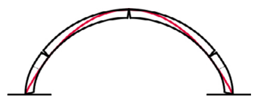	
1.50	0.12261	44.62	0.09234	48.10	0.05383	46.39
	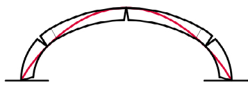		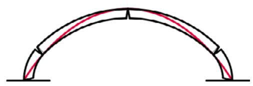		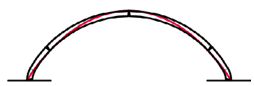	
1.75	0.11689	41.96	0.07163	46.06		
						
2.00	0.10683	39.80	0.04706	43.30		
						
2.25	0.09418	37.92				
						
2.50	0.07995	36.20				
						

Furthermore, minimum thickness values are computed for arches assumed in (47) as optimal, and the corresponding graph is also traced in Figure 6 (dash-double-dotted line). However, for any ratio $l{:}h$, there are arches which have a smaller minimum thickness value (e.g., compare to the graph for α=45°); hence, in (31), the criterion for arch optimality is inappropriately chosen, or it can be related only to aesthetic properties.

Table 2. Limit equilibrium state of arches that have classic oval shape

classic oval shape			arch of minimum thickness			classic oval shape			arch of minimum thickness		
α [°]	$r : R$	$l : h$	t/l	t/r	β_{in} [°]	α [°]	$r : R$	$l : h$	t/l	t/r	β_{in} [°]
45	$1 : 1+\sqrt{2}$	1.414	0.09807	0.19614	48.87	30	$3-\sqrt{3} : 3$	1.423	0.12307	0.20713	45.62
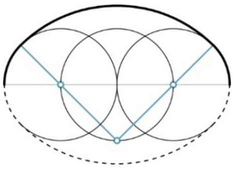			Serlio II 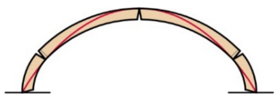			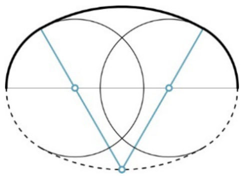			Hernán Ruiz 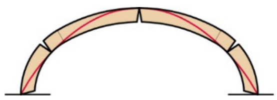		
45	1 : 2	1.414	0.10323	0.17623	49.81	30	1 : 3	1.577	0.12146	0.24291	43.72
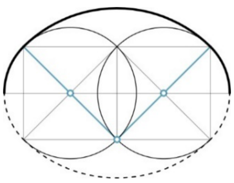			Serlio III 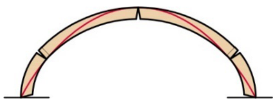			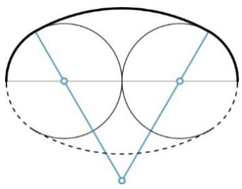			Vandelvira 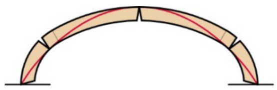		
30	1 : 2	1.323	0.12245	0.18367	47.08	26.57	1 : 2	1.309	0.12536	0.18142	46.84
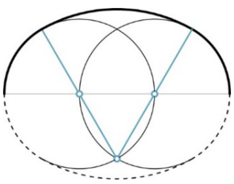			Serlio IV 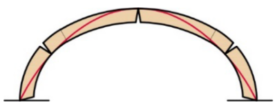			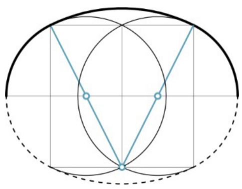			Fray Lorenzo 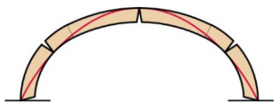		
36.87	3 : 8	1.500	0.11048	0.22095	46.06	30	1 : 4	1.783	0.11576	0.28939	41.65
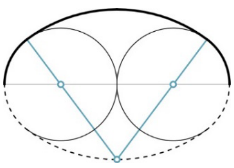			Vignola 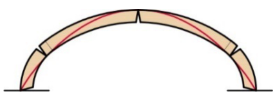			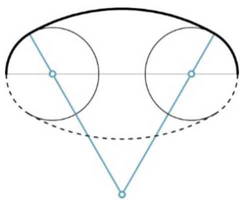			Gelabert 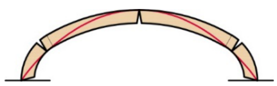		
53.13	8 : 3	0.667	0.08580	0.04290	65.13	30	2 : 1	0.804	0.08747	0.06560	62.17
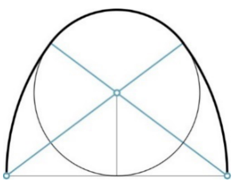			Egyptian 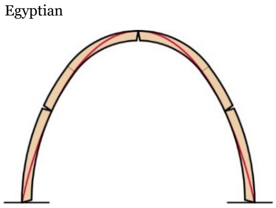			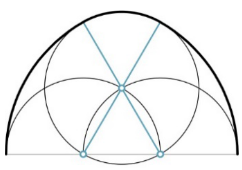			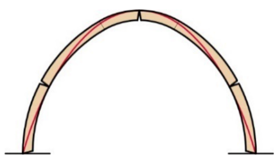		

Informes de la Construcción, Vol. 77, 578, 6921, abril-junio 2025. ISSN-L: 0020-0883. https://doi.org/10.3989/ic.6921

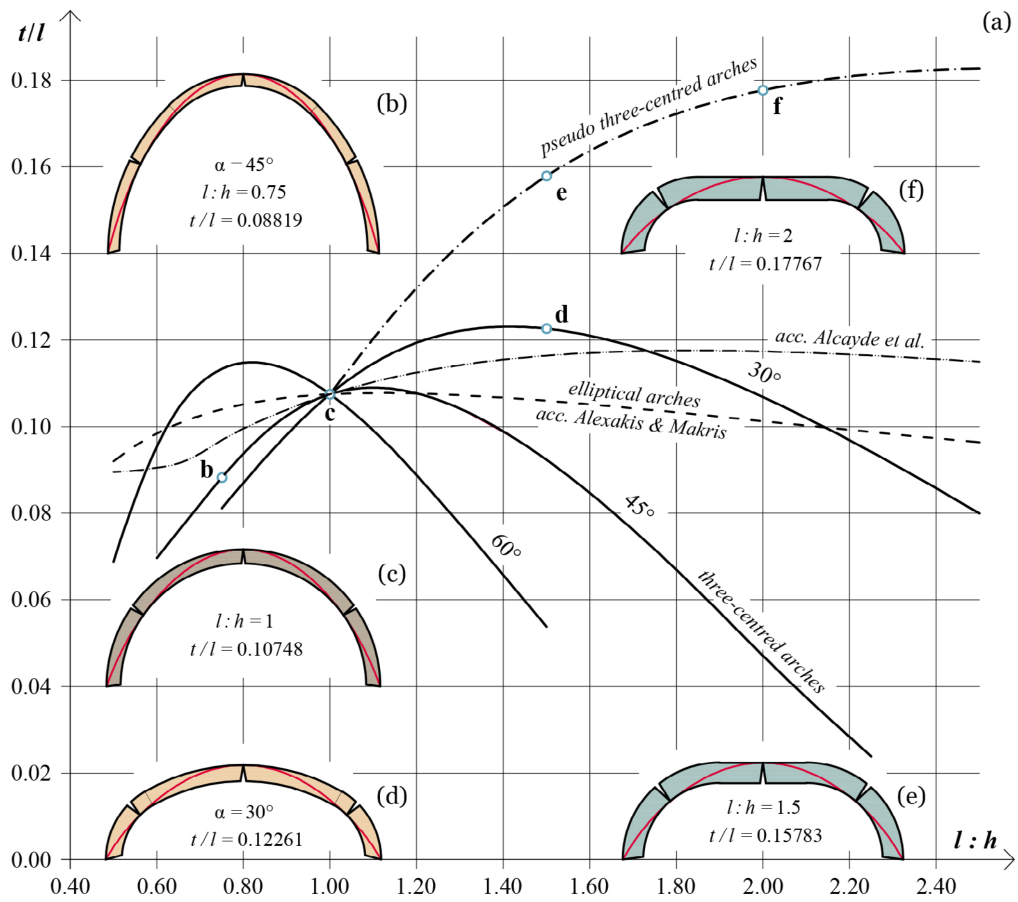

Figure 6. (a) Graph showing the correlation between the minimum thickness *t/l* and the shape of three-centred and pseudo-three-centred arch (defined by the transition angle α and the ratio *l:h* between the half-span and the arch height), (b, d) three-centred arches, (c) semicircular arch, (e, f) pseudo-three-centred arches

For various shapes of pseudo-three-centred arches, defined by the ratio between the radius r of circular part II and the half-span l (i.e., by the ratio *l:h*), values of minimum thickness *t/l* are computed and are provided in Table 3, and the corresponding graph is traced in Figure 6 (dash-dotted line). One can note that the minimum thickness value quickly increases as the ratio *l:h* increases (up to the *l:h ≈ 2.6*), while the location of the critical section (β_{in}) approaches the springings. In addition, the graphical representation of limit equilibrium state of these arches is also shown in Table 3.

Table 3. Pseudo-three-centred arches of minimum thickness

l:h	*t/l*	β_{in} [°]	β_{in} [°]	*t/l*	*l:h*
1.00	0.10748	54.48	45.67	0.13728	1.25
				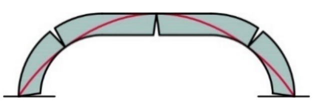	
1.50	0.15783	40.14	36.54	0.17046	1.75
	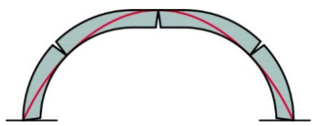			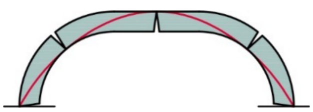	
2.00	0.17767	33.66	30.25	0.18274	2.50
	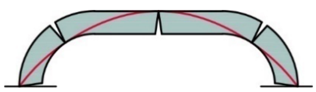			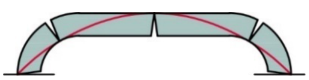	
3.00	0.18144	27.61	23.84	0.17203	4.00
					

6. CONCLUSION

Structural behaviour of three-centred and pseudo-threecentred arches, albeit they are very common in architectural heritage, has not been sufficiently researched. Hence, on the base of thrust line theory, in the present paper, complete insight into the equilibrium analysis of such arches, having a constant thickness and loaded by self-weight, is provided. Analytical modelling has been carried out according to the geometric formulation, i.e., macroscopic equilibrium analysis of a finite portion of an arch. Adopting the five-hinged collapse mode for the corresponding numerical modelling, it is shown that the previously developed method regarding critical area selection, aimed for the determination of minimum thickness value, can be adapted for the analysis of three-centred arches. Furthermore, on the base of numerical results, it is concluded that graphs correlating three-centred arch shape and the corresponding minimum thickness, where one can simultaneously consult structural and aesthetic properties, has a parabola-like shape. The visual representation of the limit equilibrium state for more than thirty arches, with the corresponding thrust line and hinges arrangement, is provided for the first time. Considering a large presence of oval arches of classic proportions, they are particularly treated. However, since the shape determination is based on purely geometrical properties, regardless of loadings, it is concluded that it can be related only to aesthetic properties but not to structural ones. Thus, it is shown that the ones the layout of which is based on the equilateral triangle (Serlio's and Vignola's method), turn out to be the most unsuitable ones, since they reach the largest value of the minimum admissible thickness.

The proposed analytical modelling is limited to symmetrical three-centred arches subjected only to self-weight. Further, it is based on the premise that analysed arches are of an idealised shape which does not suffer deformations under load. Hence, in order to provide a more direct application to stability analyses aimed for real structures, the modifications of the initial ideal geometry, as well as different loading conditions or backfill addition, remain to be considered.

Regarding the further possible developments of the present research, the conducted analysis can be used as the basis for the modelling of mechanical behaviour of circular-based arches with more centres, such as five-centred or Tudor arches.

DECLARATION OF COMPETING INTEREST

The author of this article declare that he didn't have financial, professional or personal conflicts of interest that could have inappropriately influenced this work.

FUNDING SOURCES

This research has been supported by the Ministry of Science, Technological Development and Innovation (Contract No. 451-03-137/2025-03/200156) and the Faculty of Technical Sciences, University of Novi Sad through project "Scientific and Artistic Research Work of Researchers in Teaching and Associate Positions at the Faculty of Technical Sciences, University of Novi Sad 2025" (No. 01-50/295).

AUTHORSHIP CONTRIBUTION STATEMENT

Dimitriye Nikolich: Conceptualization, Formal analysis, Funding acquisition, Investigation, Methodology, Project administration, Visualization, Writing – original draft, Writing – review & editing.

REFERENCES

(1) Benvenuto, E. (1991). *An Introduction to the History of Structural Mechanics*. New York: Springer-Verlag.
(2) Cowan, H. J. (1981). Some observations on the structural design of masonry arches and domes before the age of structural mechanics. *Architectural Science Review*, 24(4), 98–102.
(3) Radelet-de Grave, P., 2003, The use of a particular form of the parallelogram law of forces for the building of vaults (1650–1750). In Becchi, A., Corradi, M., Foce, F., Pedemonte, O., (Eds.) *Essays on the History of Mechanics* (pp. 135-163). Springer Basel AG.
(4) Sakarovitch, J., 2003, Stereotomy, a multifaceted technique. In Huerta, S. (Ed.), *Proceedings of the First International Congress on Construction History* (pp. 69-79). Madrid, Instituto Juan de Herrera, Escuela Técnica Superior de Arquitectura.
(5) Hooke, R. (1676). *A Description of Helioscopes and Some Other Instruments*. London: John Martyn.
(6) Truesdell, C. (1960). *The Rational Mechanics of Flexible or Elastic Bodies 1638-1788, Introduction to Leonhardi Euleri Opera Omnia*. Volume XI of 2nd series, Zürich: Orell Füssli.
(7) Nikolić, D., Živaljević, V. (2020). On the modelling of vaulted structures of equal strength. *Nexus Network Journal*, 22(4), 1219–1236. https://doi.org/10.1007/s00004-020-00507-y
(8) Couplet, P. (1730). Seconde partie de l'examen de la poussee des voûtes. *Histoire de l'Académie Royale des Sciences,* 1732, 117–141.
(9) Heyman, J. (1972). *Coulomb's Memoir on Statics: An Essay in the History of Civil Engineering*. Cambridge university press.
(10) Young, T. (1824) Bridge. In *Supplement to the Fourth, Fifth and Sixth Editions of the Encyclopaedia Britannica* (pp. 497–520), Volume 2, Edinburgh: Archibald Constable.
(11) Huerta, S. (2008). The Analysis of Masonry Architecture: A Historical Approach. *Architectural Science Review, 51*(4), 297–328. https://doi.org/10.3763/asre.2008.5136
(12) Moseley, H. (1843). *The Mechanical Principles of Engineering and Architecture*. London: Longman, Brown, Green and Longmans.
(13) Culmann, K. (1866). *Die graphische Statik*. Zürich: Meyer and Zeller.
(14) Heyman, J. (1997). *The Stone Skeleton: Structural Engineering of Masonry Architecture*. Cambridge University Press.
(15) Kurrer, K. E. (2018). *The History of the Theory of Structures: Searching for Equilibrium*. Berlin: Ernst & Sohn Verlag für Architectur und technische Wissenschaften GmbH & Co. KG.
(16) Milankovitch, M. (1907). Theorie der druckkurven. *Zeitschrift für Mathematik und Physik,* 55, 1–27.
(17) Foce, F. (2007). Milankovitch's theorie der druckkurven: Good mechanics for masonry architecture. *Nexus Network Journal, 9*(2), 185–210. https://doi.org/10.1007/s00004-007-0039-9

(18) Alexakis, H. and Makris, N. (2015). Limit equilibrium analysis of masonry arches. *Archive of Applied Mechanics, 85*(9), 1363–1381. https://doi.org/10.1007/s00419-014-0963-6
(19) Nikolić, D. (2019). The influence of Milankovitch's thrust line theory on the equilibrium analysis of masonry arches. In *The Life and Work of Milutin Milanković: Past, Present, Future* (pp. 58–65). Belgrade: University of Belgrade, Faculty of Architecture.
(20) Cocchetti, G., Colasante, G., and Rizzi, E. (2012). On the analysis of minimum thickness in circular masonry arches. *Applied Mechanics Reviews,* 64(5), 050802. https://doi.org/10.1115/1.4007417
(21) Alexakis, H. and Makris, N. (2013). Minimum thickness of elliptical masonry arches. *Acta Mechanica,* 224(12), 2977–2991. https://doi.org/10.1007/s00707-013-0906-2
(22) Nikolić, D. (2017). Thrust line analysis and the minimum thickness of pointed masonry arches. *Acta Mechanica,* 228(6), 2219–2236. https://doi.org/10.1007/s00707-017-1823-6
(23) Nikolich, D. (2020). Thrust line analysis of triangular arches. *Archive of Applied Mechanics*, 90, 1861–1874. https://link.springer.com/article/10.1007/s00419-020-01701-7
(24) Nikolich, D. (2020). A note on the catenary arch bending-moment-free paradox. *Meccanica*, 57, 1457–1462. https://link.springer.com/article/10.1007/s11012-022-01513-9
(25) Makris, N., Alexakis, H. (2013). The effect of stereotomy on the shape of the thrust-line and the minimum thickness of semicircular masonry arches. *Archive of Applied Mechanics*, 83, 1511–1533. https://doi.org/10.1007/s00419-013-0763-4
(26) Aita, D., Barsotti, R., Bennati, S. (2012). Equilibrium of pointed, circular, and elliptical masonry arches bearing vertical walls. *Journal of Structural Engineering,* 138(7)*,* 880–888. https://doi.org/10.1061/(ASCE)ST.1943-541X.0000522
(27) Aita, D., Barsotti, R., Bennati, S. (2019). Looking at the collapse modes of circular and pointed masonry arches through the lens of Durand-Claye's stability area method. *Archive of Applied Mechanics*, 89, 1537–1554. https://doi.org/10.1007/s00419-019-01526-z
(28) Block, P., Ciblac, T., Ochsendorf, J. (2006). Real-time limit analysis of vaulted masonry buildings. *Computers & Structures*, 84(29-30), 1841–1852. https://doi.org/10.1016/j.compstruc.2006.08.002
(29) N. Cavalagli, V. Gusella, L. Severini, (2016). Lateral loads carrying capacity and minimum thickness of circular and pointed masonry arches. *International Journal of Mechanical Sciences*, 115–116, 645-656. https://doi.org/10.1016/j.ijmecsci.2016.07.015
(30) Tempesta, G., Galassi, S. (2019). Safety evaluation of masonry arches. A numerical procedure based on the thrust line closest to the geometrical axis. *International Journal of Mechanical Sciences*, 155, 206–221. https://doi.org/10.1016/j.ijmecsci.2019.02.036.
(31) Ricci, E., Fraddosio, A., Piccioni, M.D., Sacco, E. (2019). A new numerical approach for determining optimal thrust curves of masonry arches. *European Journal of Mechanics - A/Solids*, 75, 426–442. https://doi.org/10.1016/j.euromechsol.2019.02.003.
(32) Galassi, S., Zampieri, P. (2023). A new automatic procedure for nonlinear analysis of masonry arches subjected to large support movements. *Engineering Structures*, 276, 115359. https://doi.org/10.1016/j.engstruct.2022.115359
(33) Gilbert, M. (2001). RING: A 2D rigid-block analysis program for masonry arch bridges. *ARCH'01 Third International Arch Bridges Conference*, (pp. 459–464). Paris (France).
(34) Gilbert, M. (2007). Limit analysis applied to masonry arch bridges: state-of-the-art and recent developments. *ARCH'07 – 5th International Conference on Arch Bridges*, (pp. 13–28). Madeira (Portugal)
(35) Cascini, L., Gagliardo, R., & Portioli, F. (2018). LiABlock_3D: A Software Tool for Collapse Mechanism Analysis of Historic Masonry Structures. *International Journal of Architectural Heritage*, 14(1), 75–94. https://doi.org/10.1080/15583058.2018.1509155
(36) Galassi, S., Tempesta G. (2019). The Matlab code of the method based on the Full Range Factor for assessing the safety of masonry arches. *MethodsX*, 6, 1521–1542. https://doi.org/10.1016/j.mex.2019.05.033
(37) Marmo, F. (2021). ArchLab: a MATLAB tool for the Thrust Line Analysis of masonry arches. *Curved and Layered Structures,* 8(1), 26–35. https://doi.org/10.1515/cls-2021-0003
(38) McLeana, T., Málaga-Chuquitaype, C., Kalapodis, N., Kampas, G. (2021). OpenArch: An open-source package for determining the minimum-thickness of arches under seismic loads. *SoftwareX*, 15, 100731. https://doi.org/10.1016/j.softx.2021.100731
(39) Serlio, S. (1545). Il primo libro d'Architettura, Paris.
(40) De l'Orme, P. (1568). *Le premier tome de l'architecture*. Paris: Federic Morel.
(41) Huerta, S. (2007) Oval domes: History, geometry and mechanics. *Nexus Network Journal.* 9(2), 211–248. https://doi.org/10.1007/s00004-007-0040-3
(42) Mazzotti, A. A. (2014). What Borromini might have known about ovals. Ruler and compass constructions. *Nexus Network Journal,* 16(2), 389–415. https://doi.org/10.1007/s00004-014-0190-z
(43) Mozo, A. L. (2011). Ovals for any given proportion in architecture: A layout possibly known in the sixteenth century. *Nexus Network Journal,* 13(3), 569–597. https://doi.org/10.1007/s00004-011-0083-3
(44) Rosin, P. L. (2001). On Serlio's constructions of ovals. *The Mathematical Intelligencer,* 23(1), 58–69. https://doi.org/10.1007/BF03024523
(45) Gómez-Collado, M. d. C., Roselló, V. C., and Tamborero, E. C. (2018). Mathematical modeling of oval arches. A study of the George V and Neuilly bridges. *Journal of Cultural Heritage,* 32, 144–155. https://doi.org/10.1016/j.culher.2018.01.012
(46) Huerta, S. (2004) *Arcos, bóvedas y cúpulas*. Madrid: Instituto Juan de Herrera, Escuela Técnica Superior de Arquitectura.
(47) Alcayde, A., Velilla, C., San-Antonio-Gómez, C., Peña-Fernández, A., Pérez-Romero, A., Manzano-Agugliaro, F. (2019). Basket-handle arch and its optimum symmetry generation as a structural element and keeping the aesthetic point of view. *Symmetry,* 11(10), 1243. https://doi.org/10.3390/sym11101243
(48) Fallacara, G., Resta, F., Spallucci, N., Tamboréro, L. (2011). The vault of the Hôtel de Ville in Arles. *Nexus Network Journal,* 13(3), 599–629. https://doi.org/10.1007/s00004-011-0091-3
(49) Huerta, S. (2012) Wedges and plate-bandes: mechanical theories after e la Hire. In Gargiani, R. (Ed.), *L'architrave, le plancher, la plate-forme: nouvelle Histoire de la construction* (pp. 405–435). Lausanne: Presses polytechniques et universitaires romande